

THE BELL SYSTEM TECHNICAL JOURNAL

VOLUME XXXII

JANUARY

NUMBER 1

Copyright, 1953, American Telephone and Telegraph Company

Surface Properties of Germanium

By WALTER H. BRATTAIN* and JOHN BARDEEN†

(Manuscript received September 3, 1952)

The contact potential (c.p.) and the change of contact potential with illumination $(\Delta c.p.)_L$ of several germanium surfaces have been measured. The reference electrode used was platinum. It was found that the c.p. could be cycled between two extremes about 0.5 volts apart by changing the gaseous ambient. Ozone or peroxide vapors gave the c.p. extreme corresponding to the largest dipole at the Ge surface. Vapors with OH radicals produced the other extreme. There is a one to one correlation between c.p. and $(\Delta c.p.)_L$. For 12-ohm cm n-type Ge $(\Delta c.p.)_L$ was large and positive when the surface dipole was largest, decreased to zero and became slightly negative as the surface dipole decreased to its smallest value. The variation for 12-ohm cm p-type Ge was just opposite as regards both sign and dependence on surface dipole. The surface recombination velocity was found to be independent of c.p. For a chemically prepared surface it was 50–70 cm/sec and 180–200 cm/sec for n and p-type surfaces respectively. A theory is given that explains the results in terms of surface traps, N_a per cm^2 donor-type traps near the conduction band and N_b per cm^2 acceptor-type traps near the filled band. A quantitative fit with experiment is obtained with only one free parameter. The results are direct evidence for the existence of a space charge layer at the free surface of a semiconductor.

INTRODUCTION

Every one is familiar with the fact that it is necessary to expend energy to remove an electron from a conducting solid. This energy is

* Bell Telephone Laboratories.

† University of Illinois. The contributions of the second author to this work started while he was a Member of the Technical Staff of Bell Telephone Laboratories and continued at the University of Illinois.

called the work function. The work function is caused in part by a charged double layer or dipole at the solid surface. In metals this dipole extends over a distance of the order of 10^{-8} cm. In semiconductors however part of the dipole extends into the semiconductor to a distance of the order of 10^{-6} to 10^{-4} cm depending on the properties of the semiconductor. This part of the surface dipole is called the space-charge layer. The rest of the surface dipole has approximately the same extent as in metals.

In the space between any two conducting solids there is a contact potential caused by the difference between the work functions of the two surfaces. One can measure this contact potential by several methods. We have used an adaptation of the well known method of Kelvin. If one has a reference electrode whose work function remains constant, then by measuring the c.p. between this electrode and another surface one can measure any changes in work function or total dipole of this second surface.

The above method has been used to study the properties of the germanium surface in a gaseous ambient at atmospheric pressure. It has been found that the total dipole at the germanium surface can be changed by changing the ambient and further that by proper control of the ambient the surface can be cycled back and forth between two extremes of small or large dipole corresponding to a c.p. change or work function difference of the order of one-half volt.

If one upsets the thermal equilibrium in the germanium by creating excess electron-hole pairs near the surface, the potential of the surface will change until a steady state is reached. When the extra electron-hole pairs are introduced by illuminating the surface with light, the potential change shows up as a measurable change in contact potential between the reference electrode and the Ge surface.¹ It has been found that this contact potential change on illumination $(\Delta c.p.)_L$ is large and positive on *n*-type Ge when the surface dipole is large, then decreases to zero and becomes slightly negative as the surface dipole decreases to the smaller extreme. For *p*-type Ge the $(\Delta c.p.)_L$ is large and negative when the surface dipole is small and goes through zero and becomes slightly positive as the surface dipole increases to the larger extreme.

One can describe qualitatively what is going on as follows. The extra hole and electron pairs created by the light diffuse either to the interior or to the surface to recombine. The recombination in the interior is governed by the body life time τ . The surface recombination is characterized by a recombination velocity v_s . When the surface is illuminated its potential, with respect to the interior, changes until the combined

flow of holes and electrons to the surface and interior is just equal to the rate they are being created by the light. The sign and magnitude of the potential change for a given illumination depends on the body properties of the germanium and on the size of the space charge layer.

These experimental results are direct evidence for the existence of a space charge layer at the free surface of a semiconductor. They not only confirm the results obtained for silicon surfaces¹ but go much further in that they enable one to determine how the layer is changed by the gaseous ambient used.

It is known that the surface recombination velocity, v_s , can be changed, by large factors, by surface treatment.² For mechanically treated surfaces v_s approaches thermal velocities. Every hole or electron striking the surface recombines. For such a surface it is found that $(\Delta c.p.)_L$ is too small to be measured. On the other hand v_s can be as low as 100 cm/sec for chemically polished or etched surfaces such as those used in the experiments where $(\Delta c.p.)_L$ was measured. In this case one wishes to know how v_s depends on the gaseous ambient. This was measured for the same surface used in measuring $(\Delta c.p.)_L$ and it was found that, for the ambients used, v_s is approximately a constant and therefore independent of the other surface changes.

A quantitative theory, some details of which are in the Appendix, has been formulated to explain the results. It is proposed that there are two types of recombination traps at the surface: donor type, N_a per cm^2 , with energies, E_a , near the conduction band and acceptor type, N_b per cm^2 , with energies, E_b , near the filled band. Surface recombination takes place by electrons and holes successively going into one of the two types of traps. To account for the fact that v_s is unchanged by changes in ambient, it is assumed that the concentrations of these traps are independent of ambient. Changes in c.p. with ambient are assumed to result from adsorption and desorption of fixed ions which are at an effective distance $\ell \sim 2 \times 10^{-7}$ cm outward from the surface traps. A schematic energy level diagram is given in Fig. 13, to be discussed later.

The charge of the ions is compensated mainly by charges in the surface traps which, together with the ions, form a double layer. A large part of the change in c.p. with ambient results from changes in this double layer. There is also a change in barrier height, $-eV_B$, associated with the redistribution of electrons in the traps. An increase in negative ions on the surface requires a decrease in number of electrons in traps, and thus a higher barrier.

Part of the change with light, $(\Delta c.p.)_L$, occurs in the body of the semiconductor and part occurs across the barrier layer. Changes in V_B

and occupancy of the traps compensate in their effect on surface recombination, so that v_s is unchanged by ambient. This means that changes in concentrations of electrons and holes in the interior with illumination and thus the body contribution to $(\Delta c.p.)_L$ are independent of ambient. Changes in $(\Delta c.p.)_L$ with ambient result solely from changes in V_B and are in the directions we have described earlier.

The concentrations of carriers, n and p , and their change with light are obtained as follows. Drift mobilities, μ_n and μ_p , and the equilibrium product, np , are known from earlier experiments of G. L. Pearson, J. R. Haynes and W. Shockley.³ From these, and the resistivity of the sample, which was measured, n and p can be determined. The light source is calibrated in terms of hole-electron pairs created per cm^2 per sec. The recombination rate is determined from the body life time τ and the surface recombination velocity. From these latter three measurements, one can calculate the steady state density of electrons and holes near the surface when it is illuminated.

Mention should be made here of the fact that oxygen has been found to play a definite role on the Ge surface. The large extreme in dipole is obtained when active oxygen (ozone) is introduced into the gaseous ambient. Peroxide vapors have the same effect. The other extreme is produced by vapors having an OH radical, water vapor, alcohol etc. A number of vapors not falling in either of the above classes have little or no effect on the surface dipole. Another result is that the difference in work function or dipole between n - and p -type Ge is small. This is to be expected from previous work.

We shall first discuss the experimental technique and then give the experimental results. The main conclusions of the theory will then be outlined and compared with these results.

EXPERIMENTAL METHOD

The Ge surface to be measured and the reference electrode are mounted under a bell jar. Oxygen or nitrogen as desired is allowed to flow through the bell jar at a rate of approximately 2 liters per min. The volume of the bell jar is 16 liters. The gas used flows over a drying column of silica-gel and then calcium chloride. Means are provided for bubbling this gas through any desired liquid before it enters the bell jar. A spark discharge can be run in the gas flow line. The reference electrode is placed parallel to the Ge surface about 1 mm away. It is mounted on a vibrating reed which is driven, electromagnetically, at its resonant frequency of about 90 cycles per second and at an amplitude of the order of 0.1 mm. This varies the capacity sinusoidally giving rise to an electrical signal when any potential,

contact or other, exists between the surfaces. When the proper dc potential is applied between the surfaces this signal goes to zero. If no other potentials are present this dc potential is equal and opposite to the contact potential. A phase reference method* is employed to determine this balance point with a relative accuracy of $\pm 5 \times 10^{-4}$ volts. A diagram of the Ge-reference electrode circuit is shown in Fig. 1. Care must be taken to shield this circuit. Stray capacity reduces sensitivity and should be minimized. Charged insulators inside the shield will produce an apparent c.p. All conducting surfaces other than the Ge should be relatively far from the moving reference electrode. The surface is illuminated through a compound lens system by focusing the filament image, of a suitable projection bulb, on the germanium surface. This light passes through the grid of the reference electrode which removes about 10 per cent of the light. The light can be modulated by a square wave chopper, so that $(\Delta c.p.)_L$ can be measured on an ac basis. Both Ta and Pt reference electrodes have been used. The Pt electrode appears to be somewhat more constant. If the Ge surface is replaced by a gold electrode the contact potential difference is practically independent of the changes in the gas ambient. The arrangement is such that two samples can be mounted in the bell jar and the reference electrode moved from one to the other without opening the bell jar. In this way two surfaces can be compared, without any question arising of long time drifts in the reference electrode.

EXPERIMENTAL RESULTS

I. Change of c.p. between Ge and Pt reference electrodes as a function of the gaseous ambient

When this work was started the object was to find some means of varying the c.p. It was thought that the actual values of the c.p. would

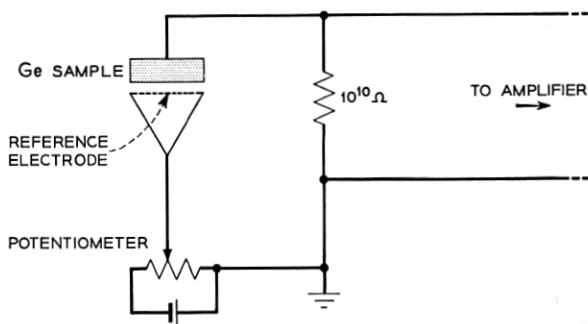


Fig. 1 — Schematic of experimental circuit.

* H. R. Moore designed and made the electronic equipment used to do this.

be highly dependent on past history of the Ge sample. If however one could measure one or more other properties, such as $(\Delta c.p.)_L$ and v_s , on the same surface at the same time, then one could look for correlations between these properties. In this manner one might be able to eliminate the past history as a factor. From previous experiments in the highly variable ambient of room air we knew the order of magnitude of the variation to be expected. At first it was impossible to produce this range of variation under the bell jar. The contact potential always drifted in the direction of a positive extreme, i.e., small total dipole at the Ge surface. The only way found to get a really large change in the opposite direction was to lift the bell jar and expose the sample to room air. These phenomena were finally traced to the presence of negative ions, possible salt ions, in the room air. These were not present in the oxygen and nitrogen supplies we used for creating the ambient in the bell jar.

It was found that the opposite c.p. extreme could be produced, under the bell jar, by running a spark discharge in dry oxygen as it was flowing into the system. The next step was to cycle the c.p. from one extreme to the other and back again. The procedure was to start with the spark discharge in dry oxygen, change to either wet O_2 or wet N_2 and to end with dry O_2 . The development of this dependable and reproducible cycle was a great aid to the proposed study. Fig. 2 is a plot of contact potential versus time for a single crystal slice D of Ge cut from a melt that was p -type. The surface was prepared by removing some of the Ge with a silicon carbide (180 mesh) blast of approximately ten pounds air pressure. The Ge was then mounted in the bell jar within one-half minute of the "sandblast," and the dry O_2 flow started. The c.p. was followed for a few minutes to be sure everything was working properly.

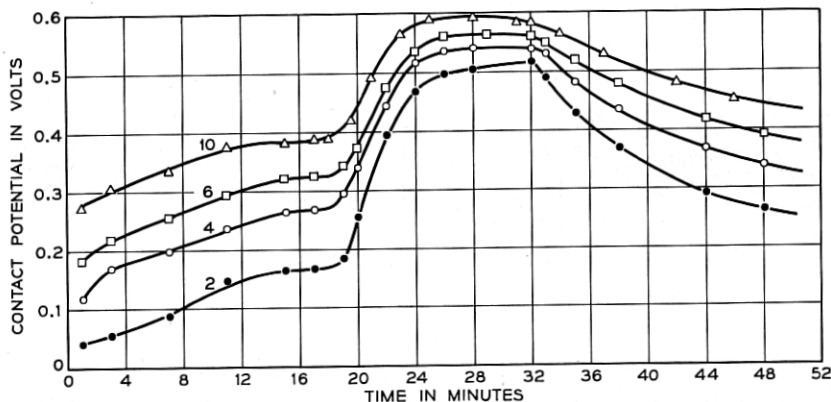


Fig. 2 — Contact potential cycles for sandblasted sample D.

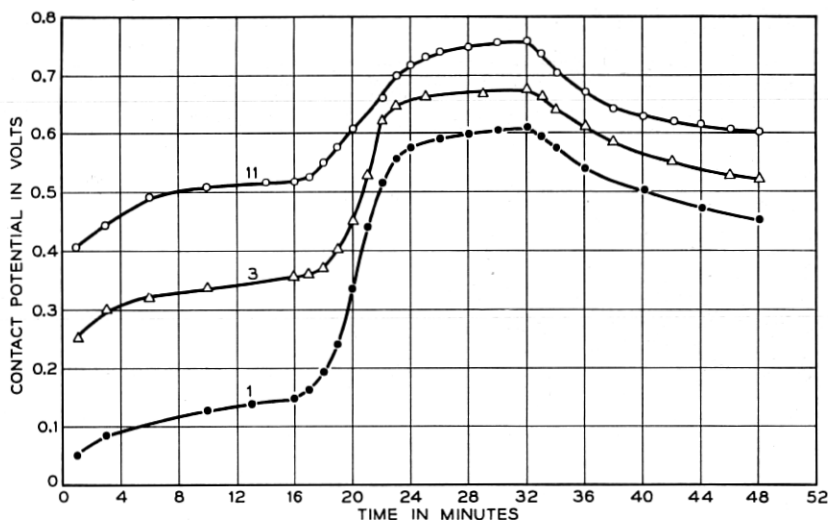


Fig. 3 — Contact potential cycles for etched sample A.

In Fig. 2 zero time is taken after the spark discharge was run in the O_2 flow line for 2 minutes. This started the first cycle. After approximately 17 minutes the O_2 was made to bubble through H_2O . Fifteen minutes or so later the O_2 was changed back to dry. At this time, 32 minutes, the flow rate was increased by a factor of three. The c.p. was followed for about 17 minutes, then the process was repeated. The results and the reason for the choice of time intervals, are all evident from a study of Fig. 2. The spark discharge in O_2 decreases the c.p. After this treatment the c.p. increases with time, most of the change occurring in the first 15 minutes. The wet O_2 then increases the c.p. to a maximum value which is reached in about 15 minutes. Finally the dry O_2 reduces the c.p. It is evident that there is a quasi-equilibrium value of c.p. in dry O_2 , to which the c.p. returns after either extreme treatment. At first there is quite a large shift from cycle to cycle but this shift gradually disappears as the cycling is continued. In Fig. 2 cycles 2, 4, 6 and 10 are shown. Very little change takes place after cycle 10. Such results have been obtained many times over a period of two years. When allowance is made for shifts in work function of the reference electrode and for the fact that the experimental technique improved as the work progressed it is found that all the results for a given sample of Ge are very consistent.

In Fig. 3 are shown similar results for an n -type slice A. In this case the surface was first ground or sandblasted to remove any films, and

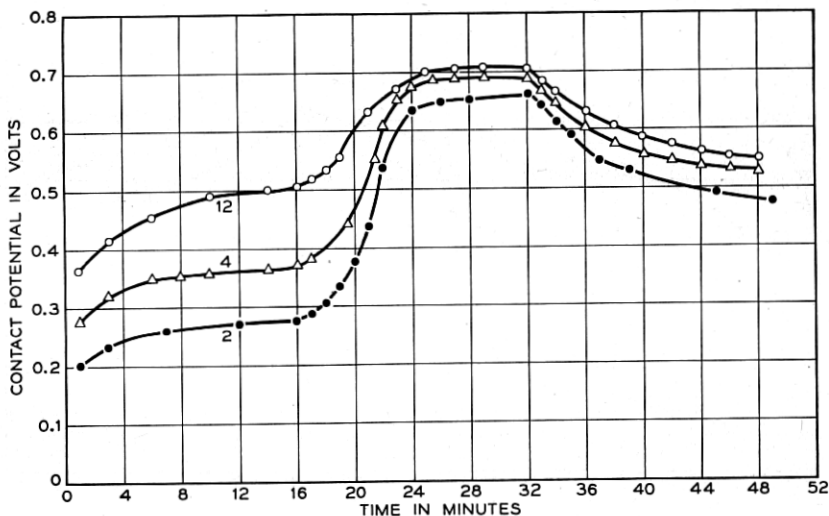


Fig. 4 — Contact potential cycles for etched sample D.

then given a polishing etch (CP-4). After the etch the surface was washed in running distilled water of reasonable quality. The surface was then dried with filter paper and kept covered until placed in the bell jar.⁴ From here on the procedure was the same as before. In this case cycles 1, 3 and 11 are shown. The surprising result is the similarity between Fig. 2 and Fig. 3. To a first approximation one is tempted to say that the dipole of a Ge surface, in the bell jar atmosphere is independent of past history. Within certain limits this is approximately true. There are differences between Fig. 2 and Fig. 3 but they are small and probably due to differences in surface treatment. Fig. 4 shows the results for *p*-type slice, D, when this surface is etched as above. This slice and the slice A were placed in the bell jar at the same time. Cycle 1, Fig. 3, was taken on A, cycle 2, Fig. 4, on D and so on. Any differences between the results in these two figures are to be attributed to the differences in samples. They cannot very well be ascribed to the reference electrode and the initial surface treatments were as nearly the same as they could be made with reasonable care. By making runs of this type two samples at a time, different samples and different surface treatments can be intercompared. This method eliminates the shifts in the work function of the reference electrode that sometimes occur from run to run. Such results can be illustrated by plotting the data for different samples and different surface treatments for cycles 10 or greater where the results for successive cycles are the same. This has been done in Fig.

5 where one cycle each is plotted for both sample A and D, for each of the two surface treatments, sandblasting and etching. The curves are approximately all of the same shape so that the differences between them can be described by giving the shift in contact potential necessary to superimpose the curves. This treatment works very well except for the first part of the cycle after the spark coil where the shift necessary is sometimes more and sometimes less than that needed to make all of two curves superimpose well. Note in Fig. 5 that the contact potential for sample A etched is always greater than for sample D etched. In the case of the sandblasted surface just the reverse is true. Also the contact potential for the etched surface of either sample is always larger than for the sandblasted.

Using these methods comparable results were obtained on two other *n*-type samples, C and E, of increasingly lower specific resistance. Taking advantage of the relation between carrier concentration and the position of the Fermi level we have plotted in Fig. 6, the contact potential for both the etched and the sandblasted surfaces versus the position of the Fermi level ($E_F - E_i$) in electron volts. The contact potential values used were taken from the saturation values in wet O_2 but the shapes of the curves would be much the same for any other point in the cycle. The contact potentials are thought to be accurate to about 0.01 volts. Solid lines have been drawn through the points. Note that the contact potential for the etched surface is always greater than for the sandblasted surface, i.e., the work function is always less and that this difference is greater when $E_F = E_i$ or the germanium is nearly intrinsic.

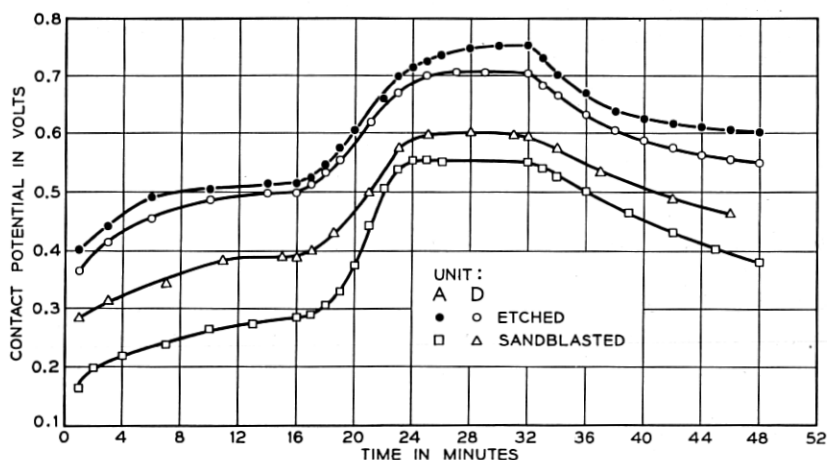


Fig. 5 — Comparison of cycles for samples A and D with sandblasted and etched surfaces.

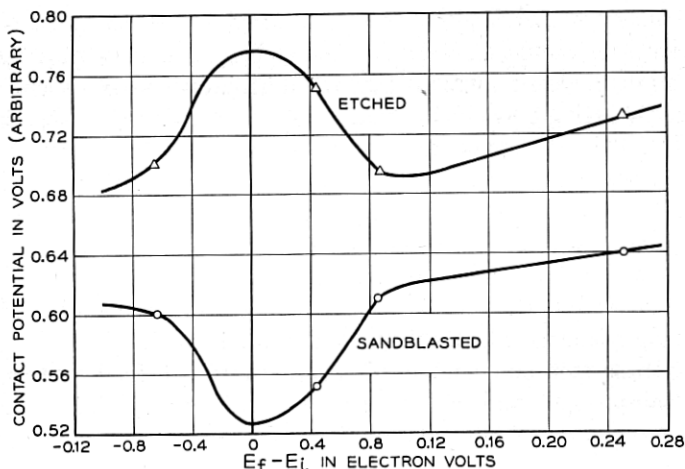


Fig. 6 — Contact potential dependence on position of the fermi level.

For variety Fig. 7 shows results on c.p. for a sandblasted polycrystalline sample of silicon. It is apparent that similar phenomena are taking place on the silicon surface, however the behavior is different. These preliminary results are shown to illustrate the generality of this method for investigating semiconductor surfaces in a controlled gaseous ambient.

The time between cycles was somewhat variable. The first and second cycles were always taken immediately after the specimen was placed in the bell jar. After this, successive cycles were taken one or two a day over a period of a week or more. The bell jar was not opened during a run and a small flow of dry gas was maintained between cycles. Little if anything occurred during these idle periods, showing that the changes that did take place were due to the cycling.

II. Change of contact potential with illumination

When the Ge surface is sandblasted the change of contact potential with illumination $(\Delta c.p.)_L$ is too small to be measured. If however the surface has been prepared by the polishing etch, the $(\Delta c.p.)_L$ is easily observed. This change if not too small can be measured by finding the balance on the potentiometer for light off and light on. When the contact potential is changing with time, or if the change is small this is difficult to do. A better procedure is to chop the light at a definite frequency and measure the amplified output on an ac meter. This gives a continuous reading that can be read easily at any given time. If a filter is used to pass only those frequencies near the fundamental of

the chopping frequency, the improvement in signal to noise enables one to read very small changes.

A plot of $(\Delta c.p.)_L$ in volts versus the contact potential for samples A *n*-type and D *p*-type is shown in Fig. 8. For the *n*-type sample the signal is large and positive when the contact potential is small and becomes small and negative as the contact potential increases. Except for the shift in the contact potential where $(\Delta c.p.)_L$ goes through zero, the results for the *p*-type sample are practically the opposite of those for the *n*-type sample. Similar curves have been obtained cycle after cycle in many complete runs. Within experimental error the curves have the same shape for a given sample for all cycles in all runs. Sometimes the curve for the first cycle in a run will differ in shape from the rest. However there are shifts such that the c.p. for which the light goes through zero $(c.p.)_0$ does vary from cycle to cycle throughout a run. Fig. 9 is a plot of $(c.p.)_0$ versus cycle number for *p*-type sample D and *n*-type sample A. The data are plotted for two distinct runs. Both of these units were in the bell jar when the measurements were taken. Consistent results of this kind give one confidence that the Pt reference electrode is staying constant.

These experimental results can be summarized as follows. All data for a given sample can be superimposed by shifts in contact potential scales for the different cycles. A plot of $(\Delta c.p.)_L$ versus $c.p. - (c.p.)_0$ can be represented by a single curve for each unit. Moreover all the curves for all units both *n*- and *p*-type have quite similar shapes provided in the latter we plot $[-(\Delta c.p.)_L]$ versus $(c.p.)_0 - c.p.$ The shape of this curve is shown in Fig. 8 for a given sample and Fig. 9 shows how $(c.p.)_0$ varies from cycle to cycle. These plots adequately describe the results.

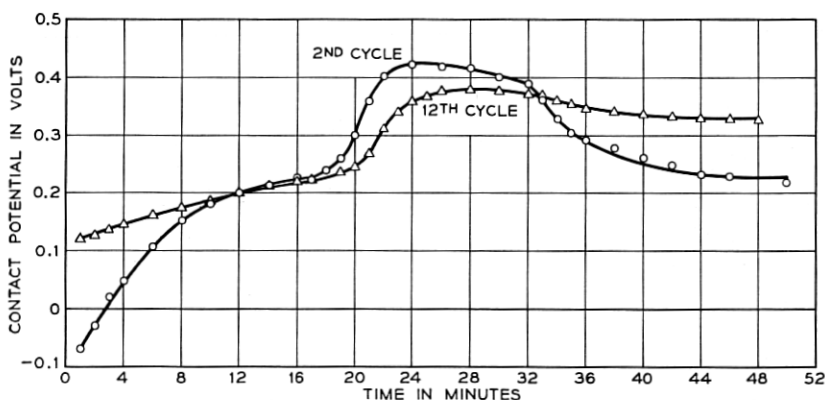


Fig. 7 — Contact potential cycles for silicon.

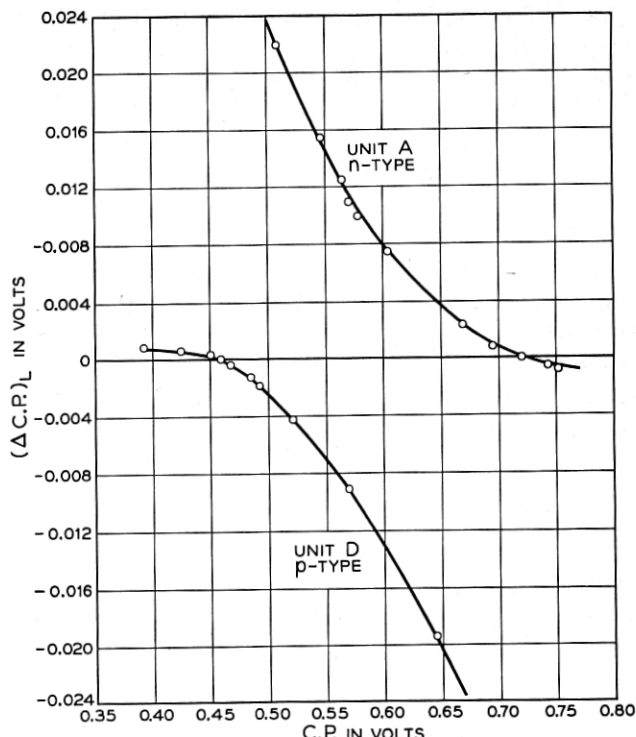


Fig. 8 — Change of contact potential with illumination versus contact potential, samples A and D etched.

Not shown in Fig. 8 because of the scale used is the result that $(\Delta c.p.)_L$ for *n*-type material does not increase indefinitely as c.p. decreases but approaches a maximum value. Likewise $-(\Delta c.p.)_L$ for *p*-type approaches a maximum as c.p. increases. Figures illustrating these results will be discussed after the theory is presented.

Some of the experimental details require discussion. It is necessary to calibrate the ac response in terms of absolute potential change. This can be done by comparing the ac reading with the dc reading when the light signal is large. One can also do this by introducing a known square-wave signal across the potentiometer in Fig. 1, and reading the ac signal out. Both methods agree when allowance is made for variation of the light signal with frequency. The latter response is almost flat from 25 to 300 cycles, but there is evidence for some very low frequency components in the dc measurements of $(\Delta c.p.)_L$. When the light signal goes through zero the signal is small and the dc value is difficult to read.

At times evidence has been obtained to indicate that the dc value changed sign. At other times the dc $(\Delta c.p.)_L$ behaved as if the place where it went through zero was shifted in c.p. from the point where the ac signal goes through zero. In view of this it was necessary to prove that the ac signal was changing phase at the zero point and not just going down in the noise and then increasing again without phase change. This was done by comparing the phase of the signal with a signal from a photocell placed in the same chopped light beam. By this means it was proved conclusively that the ac light signal was actually going through zero.

Some data were obtained on change of contact potential with light on *n*-type samples C and E having progressively smaller specific resistances. It was found that $(\Delta c.p.)_L$ decreased with specific resistance. It also decreased into the noise as the contact potential was increased, so that it could not be determined if it changed sign as for samples A and D. Because of the smaller signal $(\Delta c.p.)_L$ could not be measured easily except by the ac method and so far the signal has not been calibrated properly.

Some preliminary data on *p*-type silicon indicate that $(\Delta c.p.)_L$ for this sample was negative and that it decreased as c.p. was decreased. The magnitude of $(\Delta c.p.)_L$ for the same light intensity was much larger than for germanium and so far it has not been found to go through zero and change sign in the experimental range.

III. Other methods of varying the c.p.

In some cases N_2 was used in place of O_2 . A spark discharge in the N_2 had very little effect on the c.p. On the other hand wet N_2 produced much the same effect as wet O_2 . The positive extreme in c.p. was about 0.1 volt greater in the case of wet N_2 . After the wet treatment dry N_2 was not nearly as effective as dry O_2 in reducing the c.p. to its intermediate value. This can hardly be due to a difference in dryness of the two gases since the same drying column was used in both cases. The results indicate that dry N_2 tended to leave the surface in whatever condition obtained before the dry N_2 flow was started, and that O_2 counteracts the effect of H_2O .

With dry N_2 as a carrier, other vapors were tried. A. N. Holden suggested trying a peroxide and picked out ditertiary butyl peroxide as being reasonably safe. Use of this vapor was found to produce the same changes as the spark coil in the O_2 flow. Other vapors having OH radicals such as methyl alcohol and acetic acid were found to act the same way

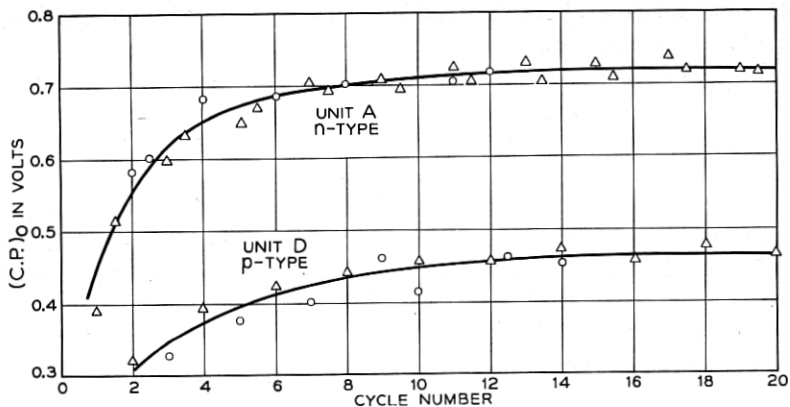


Fig. 9 — Contact potential for zero light effect, $(c.p.)_0$, versus cycle number, two runs for each sample.

as water vapor. To prove that this was not caused by traces of water in the alcohol or acid the N_2 was bubbled through water solutions of H_2SO_4 . These results indicated that one needs appreciable amounts of water vapor to produce the effect, much more than could be present in the alcohol or acid. Other vapors, such as carbon tetrachloride, methylchloride, nitrobenzene and ether, were found to have no effect on either the contact potential or $(\Delta c.p.)_L$. Acetone has a small effect in the same direction as water. This is to be expected because this compound exists in part in a tautomeric form having an OH group. Vapor from 30 per cent H_2O_2 , 70 per cent H_2O acted at first like a peroxide vapor and with a longer time of exposure behaved like water vapor. Small amounts of Cl_2 gas in N_2 produced the same change as the spark discharge in O_2 and after 14 minutes of flushing the bell jar with N_2 produced an additional effect when water vapor was introduced. On *n*-type samples before the usual increase in *c.p.* and decrease in $(\Delta c.p.)_L$ there was a large increase in $(\Delta c.p.)_L$. This was attributed to the reaction between the water vapor and the Cl left on the Ge surface, producing oxygen. The nature of the change was a rapid shift in $(\Delta c.p.)_0$ and thus a momentary increase in $(\Delta c.p.)_L$. This effect is only large in the first cycle. It indicates that the shifts in $(\Delta c.p.)_0$ plotted in Fig. 9 are probably due to an oxidation of the Ge surface as the cycling progresses. In all these experiments the relation between the *c.p.* and $(\Delta c.p.)_L$ was essentially the same as that obtained in the standard cycle.

One can detect the presence of thin surface films by electron diffraction techniques. R. D. Heidenreich took electron diffraction pictures of a germanium surface immediately after the polishing etch and water

wash. He found the surface to be quite clean, with a film thickness less than 10 \AA . He also took pictures after the germanium surface had been cycled about fifteen times and found in this case definite evidence for a thin surface film. The film was either amorphous or composed of very small crystals. He estimated the thickness to be between 20 and 50 \AA .

In the discussion of the experimental work it has been assumed that all the changes in c.p. are to be attributed to the Ge surface and not to the Pt. It is not easy to give a definite proof that this is true. The fact that it is a reasonable assumption is suggested by the nature of the results themselves. Almost identical results were obtained using a Ta electrode. In Fig. 10 we show the results of two cycles when the Ge was replaced with gold. While there are some changes they are almost an order of magnitude smaller than the changes when Ge is present. It follows that one would expect much the same results with either Ta, Pt or Au reference electrodes and that most of the changes are due to the Ge. No change of c.p. with illumination is observed when both electrodes are metals. In one case a small amount of H_2 was added to the N_2 flow. Here the c.p. between Pt and Ge changed rapidly but the $(\Delta\text{c.p.})_L$ did not change at all. Subsequent runs using the regular cycle indicated that the c.p. scale had been shifted corresponding to a reduction in work function of the Pt. Except for this shift the results were the same and the shift disappeared in about one day. The conclusion was that H_2 had little effect on Ge but reacted with the Pt decreasing its work function. This is a good illustration of the power of this method of measuring more than one property of a semiconductor surface at the same time. If only c.p. had been measured the conclusions would not have been so clear cut.

If one knew the work function of the Pt electrode then one would know the work function of the Ge. Work functions are all measured in high vacuum. We have not been able to think of a method of determining the work function of any electrode in a gaseous ambient unam-

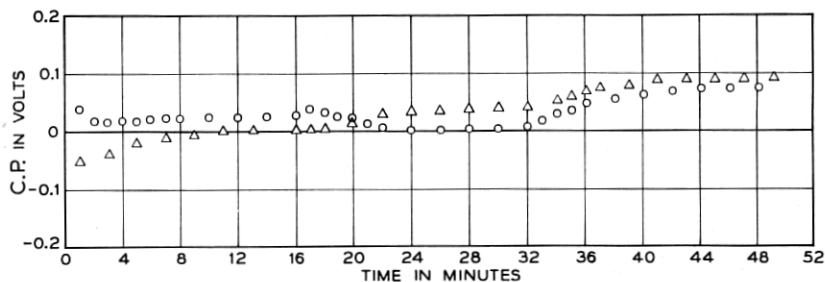


Fig. 10 — Contact potential cycles when germanium is replaced by gold.

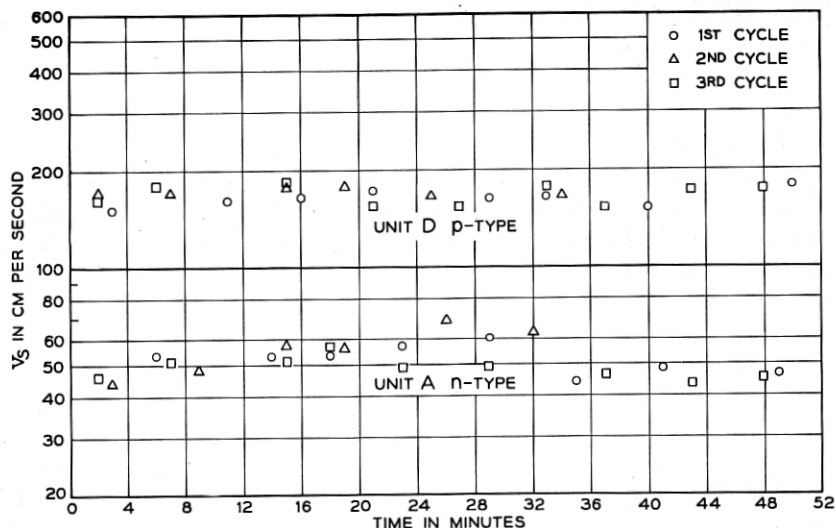


Fig. 11 — Dependence of the velocity of recombination, v_s , on the contact potential cycles.

biguously. It may well be impossible to do this in Bridgman's operational sense. Most physicists would agree that the Pt reference electrode probably has a work function of around 5 to 7 volts under these conditions, but this of course does not help much.

IV. Measurement of surface recombination velocity v_s

At first we tried various methods of measuring v_s on the Ge surface at the same time that c.p. and $(\Delta c.p.)_L$ were measured. No method was found that could be trusted. As the study progressed we realized that the c.p. of a Ge surface could be cycled in a reproducible way. Since the proper geometry for measuring v_s was a rod or filament,² rods were prepared of samples A and D with the same chemical surface treatment. The decay of hole electron pairs, created by a point light source, was measured as a function of distance from the light. If the body life time τ and the dimensions of the filament are known one can then determine v_s .² These measurements were made while the gaseous ambient was cycled in the same manner as before. The results for filaments cut from samples A and D are plotted against time in Fig. 11. The ambient atmosphere was changed as a function of time just as it was in Figs. 2 to 4. The main conclusion is that within the accuracy of this experiment there is no evident dependence of v_s on the changes in

gas ambient and therefore no dependence on the corresponding changes in surface dipole. This result was somewhat unexpected and the first time the experiment was performed it was hard to believe that the previously measured changes in c.p. actually were taking place. In this case the gas ambient was experimented with to try to change v_s and it was found that v_s could be changed from the order of 10^2 cm/sec to greater than 10^5 cm/sec and back again by exposure of the filament to $(\text{NH})_4\text{OH}$ fumes and then HCl fumes respectively.⁵ While interesting, this has no direct bearing on the other experiments. The experiment was performed again with freshly prepared rods and this time the cycling used in the c.p. experiments was rigidly adhered to, giving v_s equal to 70 cm/sec and 200 cm/sec approximately for samples A and D respectively. The experiments were then repeated again using new filaments cut from the samples as close as possible to the surfaces used in the c.p. experiments leading to the results shown in Fig. 11, namely, v_s equal to 50 cm/sec and 170 cm/sec respectively. From these experiments it was concluded that v_s is approximately constant in the range involved and is determined by the nature of the sample and the surface treatment used. It was noted in some of these experiments that v_s for the first cycle was somewhat larger than for the subsequent cycles. This change when it occurred is probably to be correlated with the changes in the early cycles in the c.p. measurements. Similar measurements on sample C gave v_s equal to 1500 cm/sec. No measurements of v_s were made on samples B and E.

V. Other experimental measurements

The specific resistance of each sample was measured near the surface used in the experiments. It was approximately constant across the surface but did vary slowly with depth in some of the samples.

The body life times were measured on each sample. The thickness of the slices used was intentionally made large compared to their corresponding diffusion lengths, about 0.5 cm for A, B, C and E and about 2.0 cm for D. The mobilities were taken from J. R. Haynes³ measurements: $\mu_n = 3600$ and $\mu_p = 1700$ cm²/volt sec. There is some uncertainty as regards the exact value of the equilibrium product of holes and electrons, np , at 300°K. We have used the value 6.3×10^{26} obtained from some unpublished data of G. L. Pearson.³

The light source was calibrated by replacing the germanium sample with one of F. S. Goucher's n - p junctions.⁶ The bell jar, with everything else including the reference electrode, was left in their normal

positions. An average was taken over the filament image, and the effective area of the p - n junction was determined and allowed for. This was done for all light intensities used. Most of the experiments were performed with a fixed intensity and the averaged result for this intensity was 6.0×10^{15} , hole electron pairs per cm^2 sec. The rate of pair production was found to be proportional to the light intensity.

Since practically all the light is absorbed in a depth (10^{-4} cm or less) that is small compared to the diffusion length, it is a simple matter to calculate the steady state increase δp in hole electron pairs due to the light. The relation is

$$\delta p = N/(v_s + v_d) \quad (1)$$

where N is the rate of pair production, v_s is the velocity of recombination at the surface and v_d is the diffusion velocity for the minority carrier. Since N is proportional to light intensity it follows that δp is too.

The magnitude of $(\Delta c.p.)_L$ should depend on the light intensity. One might at first expect it to be proportional to light intensity. That this is not the case is shown by curve 1 in Fig. 12. Curve 1 is a plot of $(\Delta c.p.)_L$ versus δp for unit D on a log-log scale. A smooth curve has been drawn through the experimental points. As we shall see later, theory predicts that if $(\Delta c.p.)_L$ is large, it should be proportional to $\ln(1 + \delta p/a)$ where a is the equilibrium density of the minority carrier,

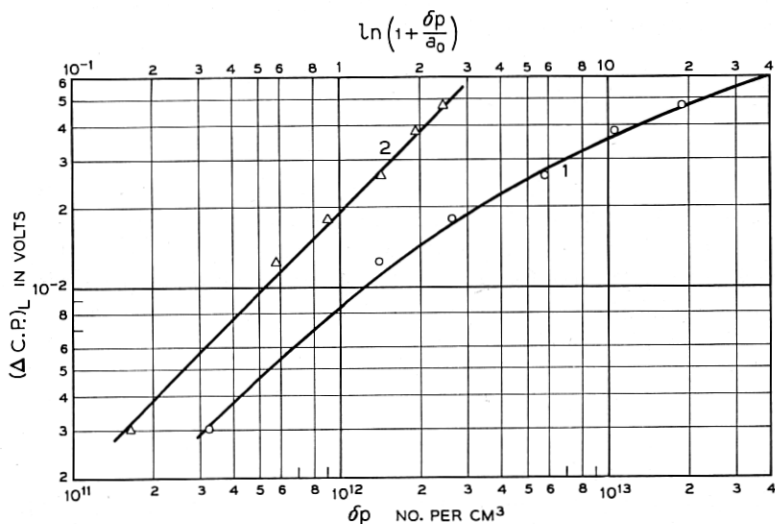


Fig. 12 — Dependence of contact potential change with illumination $(\Delta c.p.)_L$ on light intensity.

n in p -type material and p in n -type. That this prediction is borne out is shown by how well the experimental points fit the straight line curve 2 in Fig. 12 where $(\Delta c.p.)_L$ is plotted versus this quantity. The scale for δp is shown along the bottom of Fig. 12 and that for $\ln(1 + \delta p/a)$ along the top. Similar results were obtained for unit A.

In Table I the parameters, specific resistance ρ in ohm cm, life time τ in microseconds and the surface recombination velocity v_s in cm/sec are given for each unit used. Also given are some pertinent quantities derived therefrom, namely the equilibrium densities of electrons and holes, n and p in number per cm^3 and the increase in density at the surface δp in number per cm^3 when the rate of pair production due to the illumination was 6.0×10^{15} per cm^2 sec.

THEORY

The constancy of v_s throughout the range of surface dipole investigated puts rather stringent requirements on any theoretical model to be constructed. W. Shockley and W. T. Read⁷ have investigated the theory of recombination via traps. It is evident from their work that if one assumes a trap density peaked near a single energy and very small elsewhere, then v_s will be constant over a range of surface dipole values provided that the peak energy is either near the conduction band or near the filled band. The experimental results make it appear very unlikely that the trapping mechanisms on the n and p -type surfaces are essentially different. It is assumed that both types of traps are present on the surface and that the traps are approximately the same for both n - and p -type samples. Further, it is assumed that the traps N_a of energy E_a near the conduction band are donor type, i.e., neutral when filled and positively charged when empty. Likewise the traps N_b of energy E_b near the filled band are assumed to be acceptor-type traps, i.e., neutral when empty and negatively charged when filled. The absolute charge on the traps is not important, however, because we are

TABLE I

Sample	Type	ρ	n_0	p_0	τ	v_s	δp	C
A	n	12.5	1.38×10^{14}	4.56×10^{12}	900	50-70	2.2×10^{13}	4.4×10^{-13}
B	n	15	1.14×10^{14}	5.6×10^{12}	600	(100)	1.9×10^{13}	—
D	p	12.0	2.1×10^{12}	3.0×10^{14}	4000	170-200	1.75×10^{13}	6.0×10^{-13}
C	n	2.5	7.0×10^{14}	0.91×10^{12}	48	1.5×10^3	1.67×10^{12}	20.0×10^{-13}
E	n	0.008	4.4×10^{17}	1.45×10^9	—	—	—	—

concerned only with differences between the occupied and unoccupied states.

The fraction of the traps which are occupied depends on the trap energy and on the position of the Fermi level at the surface. The latter in turn depends on the condition that the surface as a whole be neutral. A very obvious mechanism for changing the total surface dipole is the adsorption or desorption of ions on the surface. If this happens the position of the Fermi level at the surface shifts until the total charge on the surface, adsorbed ions, charge in the traps and charge in space-charge layer, adds up to zero. The consequences of this model have been carried through.

The basis for the theory is illustrated in the energy level diagram of Fig. 13. At the semiconductor surface there is a space-charge layer of thickness ℓ_B which gives a change in electrostatic potential of V_B , corresponding to a potential energy of an electron of $-eV_B$. Outside of the surface of the germanium proper, there is a surface film of thickness ℓ_D . A double layer giving a potential change V_D , is formed from a charge of ions, σ_I , on the outer surface of the film and charges in the surface traps of types *a* and *b*. Changes in c.p. with ambient result from changes in σ_I and consequent changes in V_B and V_D . It is assumed that the remainder of the work function is independent of ambi-

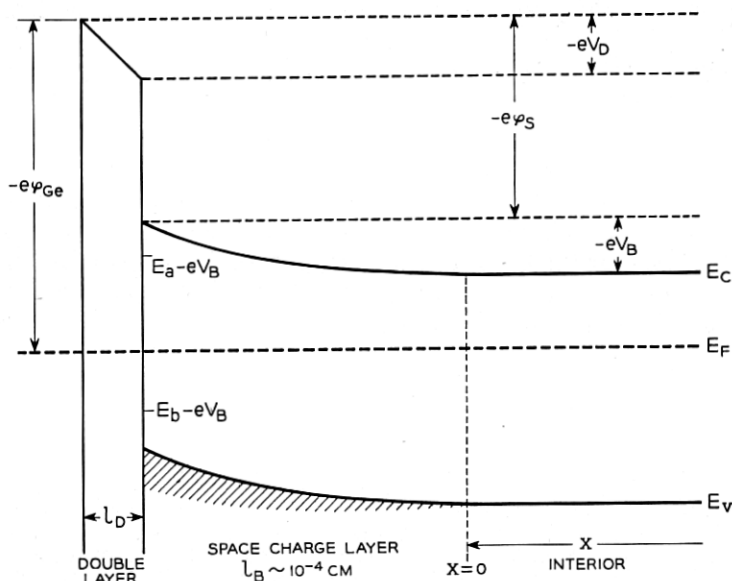


Fig. 13 — Schematic of energy level diagram at germanium surface.

ent. When light shines on the surface, V_B is changed to $V_B + \delta V_B$ and there is an additional potential drop, δV_i , in the body of the germanium resulting from the recombination current which flows to the interior. The change in contact potential with light is equal to $\delta V_B + \delta V_i$.

The film thickness ℓ_D is shown on an exaggerated scale. We expect $\ell_D \sim 10^{-6}$ cm and $\ell_B \sim 10^{-4}$ cm, so that $\ell_B \gg \ell_D$.

TABLE OF SYMBOLS

A. Energies:

E_a = E_a (true) + $kT \ln (\omega_{unoc}/\omega_{oc})$, is the effective energy of the a -traps for $V_B = 0$. Here ω_{unoc} and ω_{oc} are the statistical weights of the unoccupied and occupied states, respectively.

E_b = effective energy of the b -traps for $V_B = 0$.

E_c = energy of lowest state of conduction band in interior of semiconductor just beyond the space-charge layer.

E_v = energy of highest state of valence band at the same position.

E_F = Fermi energy.

E_i = E_F when material is intrinsic.

V_D = potential drop across surface film.

V_B = potential drop across space-charge layer.

V_{B0} = value of V_B for which $n_a = p_b$, see below.

V_0 = value of V_{B0} for an intrinsic sample.

B. Concentrations:

n = $N_c \exp [(E_F - E_c)/kT]$ = equilibrium concentration (no./cm³) of conduction electrons in interior of semiconductor just beyond the space-charge layer.

p = $N_v \exp [(E_v - E_F)/kT]$ = corresponding hole concentration.

n_i = intrinsic concentration.

n_s, p_s = equilibrium concentrations of electrons and holes, respectively, at the surface.

N_a, N_b = concentration (no./cm²) of a - and b -traps, respectively.

n_a = equilibrium concentration (no./cm²) of occupied a -traps.

p_b = $N_b - n_b$ = equilibrium concentration (no./cm²) of unoccupied b -traps.

n_{a0}, p_{b0} = values of n_a and p_b for an intrinsic sample with $V_B = 0$.

n_1 = $n + \delta n$, $p_1 = p + \delta p$, and $n_{s1}, p_{s1}, n_{a1}, p_{b1}$ = concentrations in presence of light. Electrical neutrality requires that $\delta n = \delta p$.

The theory is based on the following postulates:

I. Changes in c.p. with ambient result from changes in σ_I and the consequent changes in V_B and V_D .

$$\text{c.p.} = V_B + V_D + \text{const.} \quad (2)$$

The charge σ_I is largely compensated by charges in the surface traps. The barrier height, V_B , is determined by the requirement of electrical neutrality:

$$\sigma_I = e(n_a - p_b) + \text{const.} \quad (3)$$

Since V_B and V_D are of the same order, the net charge per unit area in the space-charge layer will be smaller than σ_I in the approximate ratio ℓ_D/ℓ_B and may be neglected.

II. Traps of type a have energies above E_F and of type b below E_F for all values of V_B attained in the different ambients used. More exactly

$$E_a - eV_B - E_F > kT, \quad (4)$$

$$E_F - E_b + eV_B > kT, \quad (5)$$

for all V_B . One may then use the Boltzmann approximations for n_a and p_b :

$$n_a = \frac{N_a}{1 + \exp [(E_a - eV_B - E_F)/kT]} \quad (6)$$

$$\sim N_a \exp [(E_F - E_a + eV_B)/kT],$$

$$p_b = \frac{N_b}{1 + \exp [(E_F - E_b + eV_B)/kT]} \quad (7)$$

$$\sim N_b \exp [(E_b - eV_B - E_F)/kT].$$

It is not necessary for our arguments to assume that all traps of each type have the same energy. The only requirement is that the distributions of trap energies are such that the a -traps are always above and the b -traps always below the Fermi level for any ambient.

III. Creation of electron-hole pairs by absorption of light occurs near the surface in a distance that is small compared with the diffusion length. Optical constants of germanium indicate that practically all of the light with energy sufficient to create electron-hole pairs is absorbed within a distance of 10^{-4} cm of the surface. The diffusion length is of the order of 0.2 cm.

IV. In the presence of light, the concentration of electrons in a -traps

is in equilibrium with the concentration of electrons in the conduction band and holes in b -traps are in equilibrium with holes in the valence band. The barrier height is adjusted so that the total charge in both types of traps is unchanged by illumination. We shall show in the appendix that the resistance to flow of electrons from the conduction band across the space-charge layer and into a -traps is small compared with the resistance to flow of electrons from the valence band to the traps. Similar considerations apply to flow of holes to b -traps from the valence band as compared with flow from the conduction band.

V. Recombination is limited by holes going into traps of type a and electrons going into traps of type b . The two types of traps act in parallel for recombination. The contributions to the surface recombination velocity are proportional to $p_s n_a$ and $n_s p_b$, respectively. These products are independent of V_B and thus of ambient if postulates II and IV are satisfied. If other types of traps were important in recombination, one would expect v_s to depend on ambient, contrary to what is observed.

Postulates I and II are used to relate V_B and c.p. with changes in ambient. Postulates III, IV, and V are used to relate $(\Delta c.p.)_L$ with V_B and the trap densities, and also to obtain an expression for the surface recombination velocity.

As V_B is made more positive, corresponding to a decrease in barrier height for electrons, n_a increases and p_b decreases. It will be convenient for the theoretical discussion to introduce the particular barrier potential V_{BO} , for which $n_a = p_b$. With use of the Boltzmann approximations in Equations (6) and (7), this gives

$$\begin{aligned} \exp [2\beta V_{BO}] &= (N_b/N_a) \exp [(E_a + E_b - 2E_F)/kT] \\ &= (p_{b0}/n_{a0})(p/n), \end{aligned} \quad (8)$$

where $\beta = e/kT$. The last form follows from the definitions of p_{b0} and n_{a0} and by noting that $\exp [2(E_i - E_F)/kT] = p/n$. We then have

$$n_a/p_b = \exp [2\beta(V_B - V_{BO})]. \quad (9)$$

As so defined, V_{BO} depends on the Fermi level and thus on the conductivity of the specimen. We shall let V_0 be the value of V_{BO} for an intrinsic specimen. From (8)

$$n_{a0}/p_{b0} = \exp [-2\beta V_0]. \quad (10)$$

If $n_{a0} = p_{b0}$, then V_0 will be zero. Postulate II sets limits on V_0 , but V_0 is otherwise undetermined in our experiments.

We shall first relate V_D and V_B . Since the electric field in the film is $4\pi\sigma_I/K_D$,

$$V_D = 4\pi\ell_D\sigma_I/K_D, \quad (11)$$

where K_D is the dielectric constant of the film. Substituting for σ_I from Equation (3) and making use of (8) and (9), we find

$$V_D = 2H \sinh \beta(V_B - V_{B0}) + \text{const}, \quad (12)$$

where

$$H = \frac{4\pi e\ell_D}{K_D} (N_a N_b \exp [(E_b - E_a)/kT])^{\frac{1}{2}} = (4\pi e\ell_D/K_D)(n_{a0}p_{b0})^{\frac{1}{2}}. \quad (13)$$

If V_D is expressed in volts and ℓ_D in cm.

$$H = 1.8 \times 10^{-6} (\ell_D/K_D)(n_{a0}p_{b0})^{\frac{1}{2}}. \quad (13a)$$

The contact potential Equation (2) may be expressed in the form

$$\text{c.p.} = V_B - V_{B0} + 2H \sinh \beta(V_B - V_{B0}) + \text{const}. \quad (14)$$

The change in contact potential with illumination results from a potential drop δV_i in the interior and a drop δV_B across the space-charge layer. The former comes from the recombination current of holes and electrons diffusing from the surface to the interior. Since electrical neutrality requires that $\delta n = \delta p$, the concentration gradients are equal. However, the mobility of electrons is greater than that of holes, so that the diffusion current of electrons is larger than that of holes by the mobility ratio "b." Since there can be no net current flow to the interior, an electric field is established which is in such a direction as to enhance the flow of holes and retard the flow of electrons. The net potential drop associated with this electric field is

$$\delta V_i = \frac{(b-1)}{\beta(b+1)} \ln \left\{ 1 + \frac{(b+1)\delta p}{bn+p} \right\} \quad (15)$$

where $\delta p = \delta n$ is the change in concentration in the interior just beyond the space-charge layer.⁸

This potential is positive for both n - and p -type material, and is independent of ambient, since δp is independent of ambient. The observed $(\Delta \text{c.p.})_L$ is generally much larger than given by (15) and is of opposite sign for n - and p -type material. To account for the observations, it is necessary to assume that the major part of the effect is associated with a space-charge layer at the free surface. We believe that the present experiments give the most convincing evidence obtained so far for the existence of such a space-charge layer.¹

The value of δV_B , the change in potential across the space-charge layer due to light, is determined by the requirement that there be no net change in charge in the surface traps, or that

$$\delta n_a = \delta p_b. \quad (16)$$

The changes δn_a and δp_b come both from changes in δp and δn and from δV_B . According to postulate IV, $n_{a1} = n_a + \delta n_a$ is in equilibrium with the conduction band and $p_{b1} = p_b + \delta p_b$ with the valence band.

We have then

$$n_{a1}/n_a = n_{s1}/n_s = (n_1/n) \exp [\beta \delta V_B], \quad (17)$$

$$p_{b1}/p_b = p_{s1}/p_s = (p_1/p) \exp [-\beta \delta V_B]. \quad (18)$$

from which it follows that

$$\delta n_a/n_a = (n_1/n) \exp [\beta \delta V_B] - 1, \quad (19)$$

$$\delta p_b/p_b = (p_1/p) \exp [-\beta \delta V_B] - 1, \quad (20)$$

$$\frac{n_a}{p_b} = \exp [2\beta(V_B - V_{B0})] = \frac{(p_1/p) \exp [-\beta \delta V_B] - 1}{(n_1/n) \exp [\beta \delta V_B] - 1}. \quad (21)$$

Equation (21) is a quadratic equation in $\exp [\beta \delta V_B]$ which may be solved to give an explicit expression for δV_B . The role of electrons and holes may be interchanged by changing the sign of δV_B and of $V_B - V_{B0}$. This accounts for the difference in behavior of n - and p -type samples. The total change with light is the sum of δV_i and δV_B :

$$(\Delta c.p.)_L = \delta V_L = \delta V_B + \delta V_i. \quad (22)$$

In the analysis of the data, δV_i is calculated theoretically from (15) with $\delta p = \delta n$ determined from (1) and δV_B is obtained from the observed $(\Delta c.p.)_L$ and δV_i using (22). Equation (21) is then used to find $V_B - V_{B0}$. A plot of c.p. $-(V_B - V_{B0})$ versus $\sinh \beta(V_B - V_{B0})$ should be a straight line with slope $2H$. An analysis of the observed data in this manner is given in the following section.

We turn finally to a discussion of the surface recombination velocity, v_s . According to postulate V, recombination is limited by flow of holes to a -traps and of conduction electrons to b -traps. The flow of holes from the valence band to a -traps (really electrons from a -traps drop into the vacant levels in the valence band corresponding to the holes) is proportional to the product of the hole concentration at the surface p_{s1} , and the concentration of electrons in a -traps, n_{a1} . The reverse flow is that of thermal generation of holes: electrons from the valence

band go into unoccupied a -traps. Since, according to postulate II, the number of unoccupied traps is nearly equal to the total number of traps, and is thus independent of δV_B and δp , the reverse flow will be practically equal to the thermal equilibrium value. If S_{pa} is the recombination cross-section for holes, the net flow of holes to a -traps is

$$U_{pa} = S_{pa}v_p(p_{s1}n_{a1} - p_s n_a)(\text{holes/cm}^2 \text{ sec}). \quad (23)$$

Here, v_p is the velocity factor which when multiplied by the concentration gives the number of holes crossing a unit area from one direction:

$$v_p = (kT/2\pi m_p)^{1/2}. \quad (24)$$

With use of the relations, $n_{a1}/n_a = n_{s1}/n_s$, $p_{b1}/p_b = p_{s1}/p_s$, from equations (17) and (18), which follow from the fact that the a -traps are in thermal equilibrium with the conduction band and the b -traps with the valence band, (23) becomes

$$U_{pa} = S_{pa}v_p(n_a/n_s)(p_{s1}n_{s1} - p_s n_s). \quad (25)$$

This expression may be simplified further. The ratio

$$\frac{n_a}{n_s} = \frac{N_a \exp [(E_F - E_a - eV_B)/kT]}{N_c \exp [(E_F - E_c - eV_B)/kT]} = \frac{N_a}{N_c} \exp \left(\frac{E_c - E_a}{kT} \right) \quad (26)$$

is independent of E_F and V_B . The ratio may be evaluated for an intrinsic specimen with $V_B = 0$, in which case $n_a = n_{a0}$ and $n_s = n_i$. Thus

$$n_a/n_s = n_{a0}/n_i. \quad (27)$$

We also have from postulate IV,

$$p_{s1}n_{s1} = p_1 n_1. \quad (28)$$

The equilibrium products are

$$p_s n_s = pn = n_i^2. \quad (29)$$

With use of (27), (28) and (29), (25) becomes

$$U_{pa} = S_{pa}v_p(n_{a0}/n_i)(p_1 n_1 - pn). \quad (30)$$

Similarly, it is found that net flow of electrons to b -traps is equal to:

$$U_{nb} = S_{nb}v_n(p_{b0}/n_i)(p_1 n_1 - pn). \quad (31)$$

The total rate of recombination is given by the sum of U_{nb} and U_{pa} and is given by an expression of the form:

$$U = U_{nb} + U_{pa} = C(p_1 n_1 - pn) = C(n + p)\delta p. \quad (32)$$

It should be noted that the coefficient C is independent of the Fermi level and thus of the conductivity of the specimen, whereas v_s is not. The relation between them is:

$$\text{For } n\text{-type} \quad C = v_s/n, \quad (33)$$

$$\text{For } p\text{-type} \quad C = v_s/p. \quad (34)$$

Values of C may be determined empirically from observed values of v_s . Referring to Table I, for sample A, $v_s = 60$ cm/sec and $n = 1.4 \times 10^{14}/\text{cm}^3$, so that $C = 4.3 \times 10^{-13}$ cm⁴/sec. For sample D, $v_s = 180$ cm/sec and $p = 3.0 \times 10^{14}/\text{cm}^3$, so that $C = 6 \times 10^{-13}$ cm⁴/sec. The values of C are approximately the same, indicating that the traps are not much different for the two specimens.

The theoretical value of C involves n_{a0} and p_{b0} . It is the product $n_a p_b = n_{a0} p_{b0}$, which is related to the parameter H and which can be estimated from empirical data. To obtain the concentrations themselves, a value must be assumed for V_0 . We have

$$n_{a0} = (n_{a0} p_{b0})^{\frac{1}{2}} \exp[-\beta V_0], \quad (35)$$

$$p_{b0} = (n_{a0} p_{b0})^{\frac{1}{2}} \exp[\beta V_0]. \quad (36)$$

As we have mentioned previously, there is no way to determine V_0 from our experiments, although postulate II sets limits on its value.

Let us for simplicity assume that $S_{nb}v_n = S_{pa}v_p = S_t v$. Then, using (35) and (36) in (30) and (32), we have

$$C = 2S_t v (n_{a0} p_{b0} / n_i^2)^{\frac{1}{2}} \cosh \beta V_0. \quad (37)$$

This equation may be used to estimate the trapping cross-section S_t for an assumed V_0 .

COMPARISON BETWEEN THEORY AND EXPERIMENT

In Fig. 14 we have plotted c.p. - (c.p.)₀ - ($V_B - V_{B0}$) versus $2 \sinh \beta(V_B - V_{B0})$ for p -type sample D, (see Table I). Each symbol represents experimental points for one cycle. Results are shown for five different cycles not all in the same run. These results are typical of all the data obtained for this sample. It is seen that these data can be fitted over most of the range by a straight line as drawn, giving a value of $H = 0.02$ e.v.

In Fig. 15 we have used the same experimental results to plot δV_L versus c.p. - (c.p.)₀. Since the experimental values of δV_L cover a range of a factor of 20 or more, a logarithmic scale was used to plot

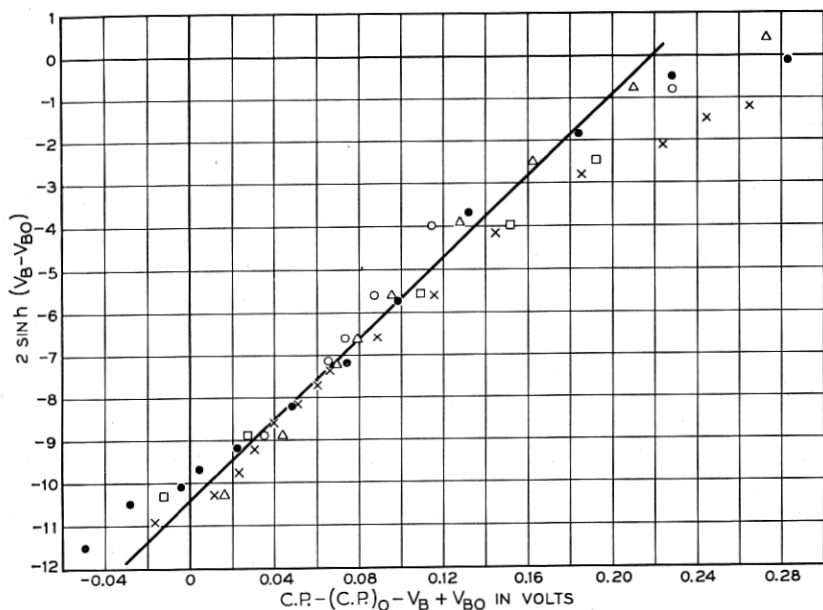


Fig. 14 — Plot of $2 \sinh \beta(V_B - V_{BO})$ versus c.p. $-(V_B - V_{BO})$ for sample D as suggested by theory.

δV_L . Both positive and negative branches of the curve are plotted on the same figure. The symbols used for the experimental points are consistent with Fig. 14. When c.p. $-(c.p.)_0$ is greater than zero, δV_L is negative. As c.p. increases it approaches a maximum negative value, this is the negative branch. When c.p. $-(c.p.)_0$ is less than zero, δV_L is positive and as c.p. decreases δV_L approaches a positive maximum value that is less in magnitude than the negative maximum. The solid curve represents the prediction of theory for $H = 0.02$ e.v. The agreement between theory and experiment is good. It should be emphasized that this fit is obtained with only one adjustable parameter.

The data for the other samples were analyzed in the same way. The results are shown by plotting δV_L versus c.p. $-(c.p.)_0$ as in Fig. 15. Fig. 16 is for n -type sample A and Fig. 17 for n -type sample B. The values obtained for H were 0.015 and 0.022 e.v. respectively. The fits obtained are about equally good in all cases with some deviation between theory and experiment near the extremes of contact potential. The values of H obtained are all of the same order as they should be if the surface trap structure is approximately the same from sample to sample. When $V_B - V_{BO}$ is large and positive and thus c.p., Eq. (14), is large, δV_L approaches the negative maximum

$$-\left[\left(\frac{1}{\beta} \ln \frac{n_1}{n}\right) - \delta V_i\right],$$

equation 21, and as $V_B - V_{B0}$ becomes small and negative, c.p. decreases and δV_L goes through zero and approaches the positive maximum

$$+\left[\left(\frac{1}{\beta} \ln \frac{p_1}{p}\right) + \delta V_i\right].$$

For p -type germanium n_1/n is greater than p_1/p so that the negative maximum for δV_L is greater than the positive maximum. Just the opposite is true for n -type germanium.

In this comparison of theory and experiment a tacit assumption has been made that the germanium surface is uniform in its properties. It might well be that this is not the case. The surface might be "patchy." To estimate what effect patches or non-uniformities might have the

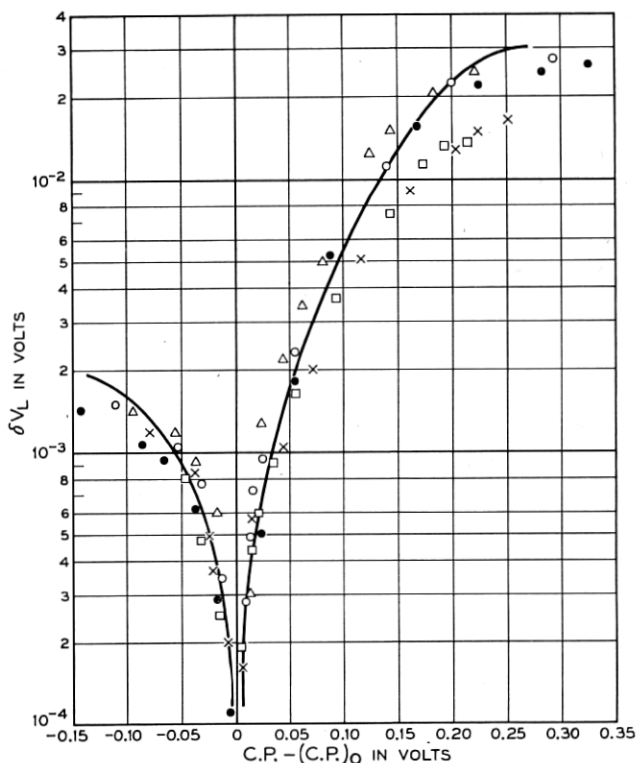


Fig. 15 — Change of contact potential with illumination, δV_L , versus c.p.; experiment and theory sample D, p -type.

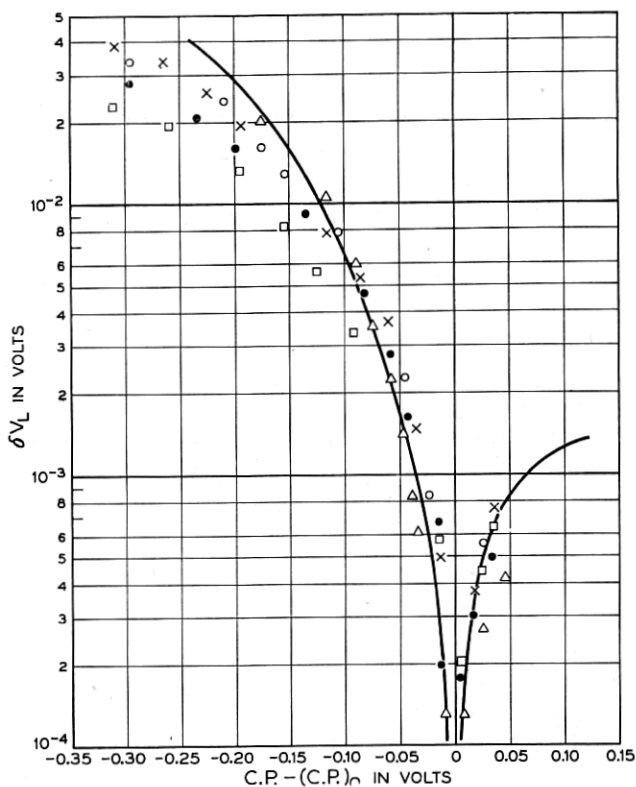


Fig. 16 — Same as Fig. 15 for sample A, *n*-type.

following was done. It was assumed that the surface was made up of two parts each having the theoretical dependence of δV_L on c.p. but with the contact potential where the light effect goes through zero differing by 0.05 volts. The values of δV_L at a given contact potential were averaged and plotted against c.p. The difference between this curve and the original one was almost entirely a simple shift in $(c.p.)_0$. It is therefore unlikely that non-uniformities in c.p., over the surface, of the order of 0.1 volts or less would change the relation between δV_L and c.p. sufficiently to be detectable.

One can use equations (8), (10) and (21) to calculate values of $(V_B - V_0)$ for each experimental value of δV_L and then plot these values against the corresponding values of contact potential. These results are shown in Fig. 18 for *n*-type sample A and *p*-type sample D. $(V_B - V_0)$ changes with c.p. as one would expect and in an approxi-

mately linear fashion throughout most of the experimental range. The change in V_B is approximately one-fifth the change in contact potential. ($V_B - V_0$) is positive for the p -type sample and negative for the n -type sample throughout most of the range. If the trap distribution on the surface were symmetrical about the intrinsic position of the Fermi level, then p_{b0} would be equal to n_{a0} and V_0 would be zero. In this case the space charge layers on n - and p -type germanium would be about equally developed. All the experimental evidence on germanium indicates that this is not the case but rather that $-V_{Bn}$ is much larger than V_{Bp} . This then means that V_0 is negative and that the trap distribution is unsymmetrical either in number or energy or both in such a way that $n_{a0} > p_{b0}$.

In Table II values are given for the differences ($V_B - V_{B0}$), etc.,

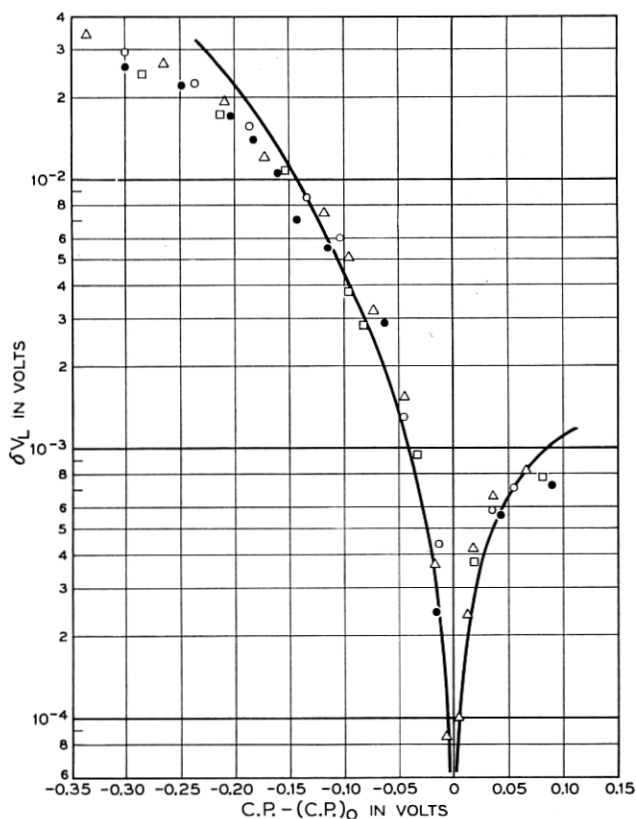


Fig. 17 — Same as Fig. 15 for sample B, n -type.

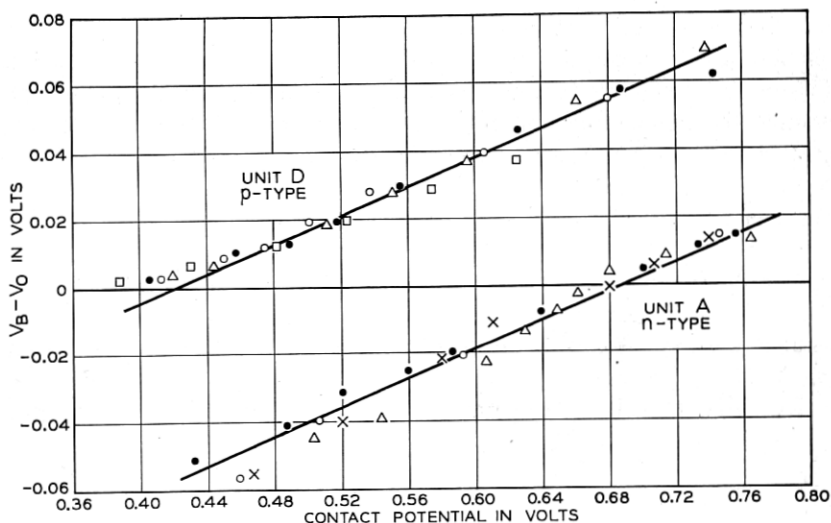


Fig. 18 — Potential across space charge layer, V_B , versus contact potential.

also δV 's, for certain special cases for samples A and D as calculated from theory. From equations (8) and (10)

$$(V_{BO} - V_0) = \frac{1}{e} (E_i - E_F) = \frac{1}{2\beta} \ln(p/n). \quad (38)$$

It is a constant for any given sample as is δV_i (see equation 15). From equations (21) and (38) it follows that when $\delta V_B = 0$ then $(V_B - V_0) = 0$ for all samples. To say this another way, if the traps are symmetrically distributed about E_i and V_B is zero, then illuminating the germanium would produce no potential difference across the surface. One would not suspect offhand that $(V_B - V_0)$ for $\delta V_L = 0$ was also approximately independent of the material in the sample but it is. For the case where δp and the minority carrier are both small compared to the majority

TABLE II

	A (n-type)	D (p-type)
$(V_{BO} - V_0)$	-0.044	+0.064
δV_i	+0.0019	+0.0015
$(V_B - V_0)\delta V_B = 0$	0	0
$(V_B - V_{BO})\delta V_B = 0$	+0.044	-0.064
$(V_B - V_0)\delta V_L = 0$	+0.010	+0.010
$(V_B - V_{BO})\delta V_L = 0$	+0.054	-0.054
$\delta V_L, (V_B - V_{BO}) = 0$	+0.024	-0.026

carrier one can easily show that when $\delta V_L = 0$,

$$(V_B - V_0) = (1/2\beta) \ln b.$$

This follows from equations (15), (21), (22) and (38). The rest of the results hardly need comment.

It is interesting to compare differences in contact potential, etc., for units A and D. In equation (2) the Fermi energy has been included in the constant. This equation predicts that if the trap distributions on both surfaces are the same, then when the contact potentials of both surfaces are equal the values of V_D should also be equal and the difference between the V_B 's should be equal and opposite to the differences between the Fermi energies in electron volts. This equation can be written

$$\text{c.p.} = (V_B - V_0) - (V_{BO} - V_0) + V_D + V_0 + \text{const.} \quad (40)$$

In comparing units we shall use Δ 's to denote differences and these differences are always taken A-D.

For the case where $\Delta \text{c.p.} = 0$, $\Delta(V_B - V_0)$ can be read from Fig. 18 and $\Delta(V_{BO} - V_0)$ from Table II. We have then

$$\Delta(V_D + V_0 + \text{const}) = -0.05.$$

This indicates that our simple picture is not quite right. If ΔV_D were zero for this case it should follow from equation (12) that both $\Delta 2H \sinh \beta(V_B - V_{BO})$ and the difference in the const in this equation should be zero. It turns out, however, that $\Delta 2H \sinh \beta(V_B - V_{BO})$ is not zero but +0.07. Equation (12) can be substituted into equation (40) giving

$$\begin{aligned} \text{c.p.} = (V_B - V_0) - (V_{BO} - V_0) + 2H \sinh \beta(V_B - V_{BO}) \\ + V_0 + \text{const}_2. \end{aligned} \quad (41)$$

Where the constant now includes the constant part of V_D and is labeled const_2 to distinguish it from the constant in equation (40). We have then for $\Delta \text{c.p.} = 0$

$$\Delta(V_0 + \text{const}_2) = -0.12.$$

This difference $\Delta(V_0 + \text{const}_2)$ can be calculated three other ways, using the experiment results and theoretical values where necessary. These ways are

1) at the same time in the cycle

$$\Delta(V_0 + \text{const}_2) = -0.10$$

2) when $\delta V_L = 0$

$$\Delta(V_0 + \text{const}_2) = -0.13$$

3) when $\delta V_B = 0$

$$\Delta(V_0 + \text{const}_2) = -0.12.$$

All four results are consistent within the probable experimental accuracy and give an average result of $\Delta(V_0 + \text{const}_2) = -0.12$ instead of zero as one might expect from the simple picture. This indicates that the trap distributions are different on the two surfaces. The constant part of V_D is proportional to $-(N_a - N_b)$ and from equation (10) one would expect V_0 to decrease as N_a increases with respect to N_b , thus ΔV_0 and Δconst_2 should be of the same sign and additive so that Δconst_2 is less than 0.12 volts; assuming that ℓ_D/K_D is the order of 2×10^{-7} cm, this indicates that $\Delta(N_a - N_b)$ is the order of 3×10^{11} per cm^2 which is small compared with the probable trap density, N_a, N_d , of the order of 10^{14} per cm^2 as we shall see in the next paragraph.

Assuming that ℓ_D/K_D in equation (13a) is the order of 2×10^{-7} cm one can calculate $(n_{a0}p_{b0})^{1/2}$ obtaining 4.1×10^{10} and 5.5×10^{10} for samples A and D respectively. Using these values one can solve for S_t in equation (37) and obtain for the case of $V_0 = 0$ the value 5.0×10^{-17} cm^2 for the average capture cross section of the surface traps. The values of S_t, n_{a0} and p_{b0} depend on what one takes for V_0 . The relations are

$$S_t = \frac{5 \times 10^{-17}}{\cosh \beta V_0},$$

$$n_{a0} = 5 \times 10^{10} \exp[-\beta V_0],$$

$$p_{b0} = 5 \times 10^{10} \exp[\beta V_0].$$

This dependence is shown in the graph in Fig. 19. As already mentioned there are reasons for thinking that V_0 is less than zero. If one takes -0.06 volts as a reasonable value then one gets $S_t = 10^{-17}$ cm^2 , $n_{a0} = 5 \times 10^{11}/\text{cm}^2$ and $p_{a0} = 5 \times 10^9/\text{cm}^2$ respectively. One can push these calculations still further to estimate N_a, N_b, E_a and E_b . One knows that E_a and $-E_b$ must be greater than $1/kT$. Also N_a and N_b should be less than the number of germanium atoms per cm^2 of surface which is $1.4 \times 10^{15}/\text{cm}^2$. Values of N_a and N_b of the order of $1 \times 10^{14}/\text{cm}^2$ for the number of traps per cm^2 with energies E_a and $-E_b$ of the order of 0.2

e.v. measured from the midband energy are reasonable and not inconsistent with the original assumptions.

As mentioned in the experimental section, some data on $(\Delta c.p.)_L$ for samples C and E have been obtained. While no complete analysis of these results has been made, one can see that they are of the right order of magnitude. As the specific resistance of the sample decreases, the body life time τ decreases. This empirical result is to be expected.⁷ Consequently δp for the same light intensity decreases and one would expect $(\Delta c.p.)_L$ to decrease as it does. For sample E of course one could not neglect the charge in the space layer so that the theory would be more involved.

The comparison between the contact potentials of samples A, C, D and E shown in Fig. 6 can be understood in part at least. Consider first the over-all result that at the same time in the cycle the c.p. for a sand-blasted surface is less than for an etched surface, i.e., the work function for the sand-blasted surface is greater. It is known that the surface recombination increases enormously when the surface is sand-blasted. This means that either the surface trap density has increased or that the distribution has changed or both in such a way as to increase surface

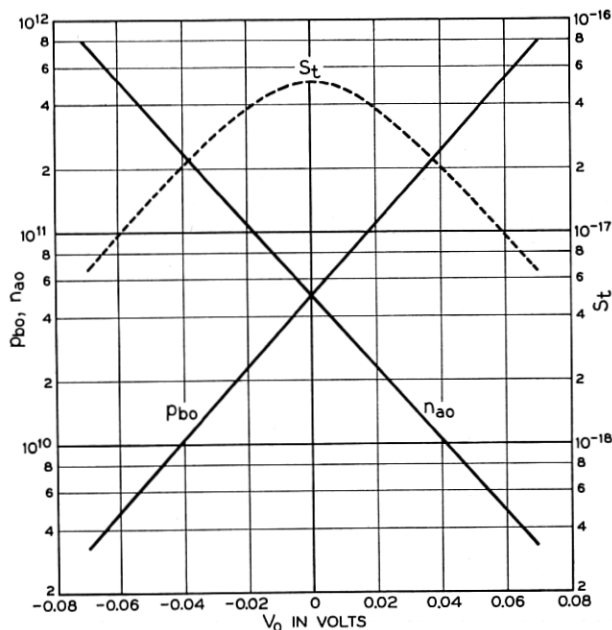


Fig. 19 — Dependence of carrier densities in surface traps, n_{a0} and P_{b0} , for $V_B = 0$, and cross section of trapping S_t on V_0 .

recombination. The results of Fig. 6 indicate that this change in trap distribution also has been in a direction to increase $(-V_B)$. This is what one would expect if N_b has increased with respect to N_a , i.e., sand-blasting increases the effective number of acceptor traps. About all that can be said about the rest of the results in Fig. 6 is that if one knew the surface trap structure in number and energy distribution for the etched surface then one could deduce from the results in Fig. 6 the distribution of traps for the sand-blasted surface over part of the energy range at least.

The theory developed here for the germanium surface may not apply at all for a silicon surface. In a previous discussion of the silicon surface¹ it was assumed that the resistance to surface trapping occurred mainly in the flow across the space charge layer rather than from the surface to the traps. This may well be the case in silicon. An investigation of the silicon surface using these same techniques should clarify this point.

It should be emphasized that the ambient used for this study and the variations in it are special in that they do not necessarily correspond to the atmosphere of ordinary room air. It is very probable that constituents in room air other than oxygen ions and water vapor are important, such as salt ions for instance. It is quite probable that v_s for such a surface exposed to room air would increase considerably with time instead of staying relatively constant as it does under the bell jar.

CONCLUSIONS

A method has been developed for studying the surface properties of Ge in a gaseous ambient at atmospheric pressure. It has been found that the Ge surface interacts with this ambient. Two atmospheric constituents that are important in this interaction, oxygen and vapors with OH radicals, have been isolated. With the controlled use of these, the surface dipole of Ge can be cycled between two extremes. Thus the dependence of other properties of the Ge surface on surface dipole, such as change of contact potential with illumination and surface recombination, can be determined.

It is evident from the results that the method is very powerful. In order to complete the present study, it was necessary to stop trying new experiments since almost all directions of variation open up new and interesting phenomena. These results on Ge are really just a beginning, and the preliminary data on silicon indicate that the same method would also be fruitful on other semiconductors. The technique is of course not limited to atmospheric pressure.

A tentative theory of the Ge surface has been developed that is sufficient to explain the experimental results on a semi-quantitative basis. Theory and the experiment together predict approximately the

number, type and distribution in energy of the surface traps. One has therefore a tentative model of the Ge surface that should be very useful in any further investigation of its properties.

ACKNOWLEDGMENTS

We wish to acknowledge the help and assistance of all our colleagues who have contributed in many ways to make this investigation a success. We wish to mention in particular E. G. Dreher and R. E.ENZ who took most of the experimental data, H. R. Moore who designed and made the electronic equipment used in making the measurements, and Conyers Herring for suggestions regarding the theory of large amplitude signals.

APPENDIX

We have assumed (Postulate IV) that traps of type *a* are in equilibrium with electrons in the conduction band and that traps of type *b* are in equilibrium with holes in the valence band. We wish to show that this is not really a separate assumption but follows as a consequence of Postulate II if the density of traps is not too high. For simplicity, we shall restrict the discussion in the appendix to the limiting case of small departures from equilibrium so that the equations are linear. The problem may then be discussed most conveniently⁷ by means of quasi-Fermi levels* or imrefs, ϕ_n and ϕ_p , for the conduction electrons and holes, respectively.

Departures $\delta\phi_n$ and $\delta\phi_p$, of the imrefs from the Fermi level are a measure of the departures of the concentrations, δn and δp , from their equilibrium values:

$$n_1 = n + \delta n = n \exp(-\beta\delta\phi_n), \quad (\text{A.1})$$

$$p_1 = p + \delta p = p \exp(\beta\delta\phi_p). \quad (\text{A.2})$$

The imrefs in the interior are then

$$\delta\phi_n = \frac{-1}{\beta} \ln \left(1 + \frac{\delta n}{n} \right), \quad (\text{A.3})$$

$$\delta\phi_p = \frac{1}{\beta} \ln \left(1 + \frac{\delta p}{p} \right). \quad (\text{A.4})$$

Correspondingly, the imrefs at the surface are defined by:

$$n_{s1} = n_s + \delta n_s = n \exp[\beta(V_B + \delta V_B - \delta\phi_{ns})], \quad (\text{A.5})$$

$$p_{s1} = p_s + \delta p_s = p \exp[-\beta(V_B + \delta V_B - \delta\phi_{ps})]. \quad (\text{A.6})$$

* Reference 2, pages 302-308.

Changes in imrefs of the traps are defined by:

$$n_{t1} = n_t + \delta n_t = \frac{N_t}{1 + \exp [(E_t - E_F - e(V_B + \delta V_B) + e\delta\phi_t)/kT]}, \quad (\text{A.7})$$

$$p_{t1} = p_t + \delta p_t = \frac{N_t}{1 + \exp [(E_F - E_t + e(V_B + \delta V_B) - e\delta\phi_t)/kT]}. \quad (\text{A.8})$$

In these last two equations, t may refer to either type of trap (a or b) and $\delta p_t = -\delta n_t$.

For small signals, the recombination current via a given set of surface traps may be considered as a flow produced by differences in the imrefs, $\delta\phi_n$ and $\delta\phi_p$, through four effective resistances in series, as shown in Fig. 20. Here R_{nB} is an effective resistance for flow of electrons across the barrier layer, R_{nt} for flow of electrons from the conduction band at the surface to the traps, R_{pt} for flow of holes from the filled band to the traps, and R_{pB} for flow of holes across the barrier layer. Under steady state conditions, the net flow of conduction electrons to the surface is balanced by an equal flow of holes. The recombination current may be thought of as a flow of electrons from the conduction band via the traps to the valence band.

The recombination current per unit area is

$$I = -eU = (\delta\phi_n - \delta\phi_p)/R_t, \quad (\text{A.9})$$

where R_t is the sum of the four resistances in series. Here U is the particle current and I is the corresponding electric current. If $\delta\phi_n$ and $\delta\phi_p$ are expressed in volts, R_t is in ohms/cm². We may define a recombination constant C_t by an equation corresponding to (34):

$$U = C_t(p_1n_1 - n_i^2). \quad (\text{A.10})$$

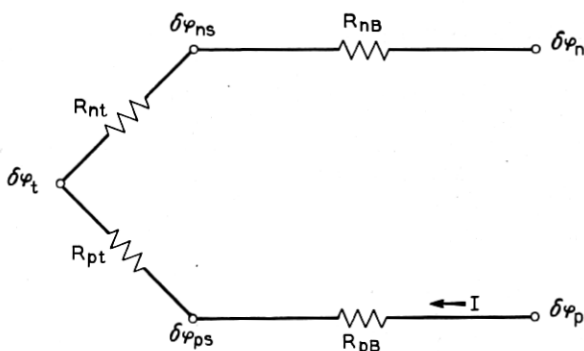


Fig. 20 — Circuit analogy of surface recombination.

The relation between C_t and R_t is obtained by use of (A.1) and (A.2) in (A.10). Since (A.9) is valid only to terms of the first order in $\delta\phi_n$ and $\delta\phi_p$, we make the corresponding approximation in (A.10) and find

$$1/R_t = e\beta n_i^2 C_t. \quad (\text{A.11})$$

If there is more than one type of trap, the net recombination resistance, R , is that of the various traps in parallel. Values obtained for R for specimens A and D from the empirical values of C are about 500 ohms.

We shall show that for a -traps, R_{pa} is much larger than the other resistances in series, and that for b -traps, R_{nb} is the dominant resistance. This implies that $\delta\phi_a = \delta\phi_n$ and $\delta\phi_b = \delta\phi_p$, or in other words that a -traps are in equilibrium with the conduction band and b -traps with the valence band.

First consider the flow across the space-charge layer. The resistances R_{nt} and R_{bt} depend on the sign of V_B . When V_B is negative, the net electron current across the space-charge layer is:

$$\begin{aligned} I &= ev_n(n_{s1} - n_1) \exp [\beta(V_B + \delta V_B)] \\ &\cong e\beta v_n n_s (\delta\phi_n - \delta\phi_{ns}), \end{aligned} \quad (\text{A.12})$$

where v_n is defined by an equation similar to (24). The second form is the linear approximation. Thus we have

$$1/R_{nB} = e\beta v_n n_s. \quad (\text{A.13})$$

If V_B is positive, n_s is replaced by n .

Correspondingly, for V_B negative, the hole current is:

$$\begin{aligned} I &= ev_p(p_{11} - p_{s1}) \exp [\beta(V_B + \delta V_B)] \\ &\cong e\beta v_p p (\delta\phi_{ps} - \delta\phi_p), \end{aligned}$$

and

$$1/R_{pB} = e\beta v_p p. \quad (\text{A.14})$$

For V_B positive, p is replaced by p_s .

The maximum value of R_{nB} is obtained for the ambient which makes V_B most negative and R_{pB} is a maximum when V_B is most positive.

The current from the conduction band to the traps is calculated as in (23):

$$I = e(v_n S_{nt} n_s p_{t1} - g_t n_{t1}) \quad (\text{A.15})$$

$$\cong e\beta v_n S_{nt} n_s p_t (\delta\phi_{ns} - \delta\phi_t). \quad (\text{A.16})$$

Here g_t is the rate of thermal generation of electrons from occupied traps to the conduction band. Since, for equilibrium conditions, $I = 0$, we have:

$$g_t = v_n S_{nt} n_s p_t / n_t. \quad (\text{A.17})$$

It may be verified easily that g_t is independent of E_F and V_B . The ratio,

$$n_{ct} = n_s p_t / n_t = N_c \exp [(E_t - E_c) / kT], \quad (\text{A.18})$$

is the equilibrium concentration of electrons in the conduction band when the Fermi level is at the level of the traps. The expression (A.16) is again the linear approximation. Thus

$$1/R_{nt} = e\beta v_n S_{nt} n_s p_t. \quad (\text{A.19})$$

Similarly, we have

$$1/R_{pt} = e\beta v_p S_{pt} p_s n_t. \quad (\text{A.20})$$

We shall show* that the ratio

$$R_{nt}/R_{pt} = (v_n S_{pt} / v_p S_{nt}) (p_s n_t / n_s p_t), \quad (\text{A.21})$$

may be expected to be small compared with unity for a -traps and large compared with unity for b -traps. First consider a -traps. If anything, $S_{pa} < S_{na}$, because holes must give up a larger energy than conduction electrons in going to a -traps. The second factor is small compared with unity if

$$p_s \ll n_{ct}, \quad (\text{A.22})$$

with n_{ct} defined by (A.18). This will be the case if the a -traps are closer to the conduction band than the top of the valence band at the surface is to the Fermi level. According to Postulate II, this should always be the case.

Similarly, for b -traps

$$R_{pt}/R_{nt} \ll 1 \quad (\text{A.23})$$

if

$$n_s \ll p_{vt}, \quad (\text{A.24})$$

where

$$p_{vt} = p_s n_t / p_t = N_v \exp [-(E_t - E_v) / kT]. \quad (\text{A.25})$$

is the concentration of holes in the valence band when the Fermi level is at the level of the traps.

The values of R_{nB} and R_{pB} relative to R_{nt} and R_{pt} are:

$$R_{nB}/R_{nt} = S_{nt}p_t \quad (\text{A.26})$$

$$R_{pB}/R_{pt} = S_{pt}n_t \quad (\text{A.27})$$

In our experiments these are always small compared with unity, since the trapping cross-sections are of the order of 10^{-17} cm² and p_t and n_t are always less than N_t , which is of the order of 10^{14} /cm².

Barrier resistances may be important for surfaces with a large number of surface traps. Analysis of earlier data on the change of the contact potential of silicon with light¹ was made on the assumption that the probability that an electron or hole reaching the surface be trapped is relatively large, and that consequently the barrier resistances are large compared with the trapping resistances. The present experiments on germanium throw doubt on this interpretation, but further experiments are required to clarify the situation.

REFERENCES

1. Bardeen, J., Phys. Rev., **71**, p. 717, 1947. Brattain, W. H., Phys. Rev., **72**, p. 345, 1947 and Semi-Conducting Materials Butterworths Scientific Publications Ltd., pp. 37-46, 1951.
2. Shockley, W., *Electrons and Holes in Semiconductors*. D. Van Nostrand, pp. 318-325, 1950.
3. Pearson, G. L., unpublished data. J. R. Haynes and W. Shockley, Phys. Rev. **81**, p. 835, 1951.
4. The CP-4 etch is due to R. D. Heidenreich. The formula is given in Phys. Rev., **81**, p. 838, 1951. This method of treating a Ge surface is due to C. S. Fuller.
5. C. S. Fuller suggested the use of these fumes.
6. Goucher, F. S., G. L. Pearson, M. Sparks, G. K. Teal and W. Shockley, Phys. Rev. **81**, p. 637, 1951.
7. Shockley, W. and W. T. Read, Phys. Rev., **87**, p. 835, 1952.
8. van Roosbroeck, W., Bell Sys. Tech. J., **29**, p. 560, 1950.